Author/s:
Gray, HA;Guan, S;Young, TJ;Dowsey, MM;Choong, PF;Pandy, MG

Title:
Comparison of posterior-stabilized, cruciate-retaining, and medial-stabilized knee implant motion during gait.

Date:
2020-08

Citation:
Gray, H. A., Guan, S., Young, T. J., Dowsey, M. M., Choong, P. F. & Pandy, M. G. (2020). Comparison of posterior-stabilized, cruciate-retaining, and medial-stabilized knee implant motion during gait.. Journal of Orthopaedic Research, 38 (8), pp.1753-1768. https://doi.org/10.1002/jor.24613.

Persistent Link:
https://hdl.handle.net/11343/275338

Hans Gray ORCID iD: 0000-0002-2587-8747

Tony Young ORCID iD: 0000-0001-9519-9195

Comparison of Posterior-stabilized, Cruciate-retaining, and Medial-stabilized Knee Implant Motion during Gait

Hans A. Gray[1], Shanyuanye Guan[1], Tony J. Young[2,3], Michelle M. Dowsey[2,3], Peter F. Choong[2,3], Marcus G. Pandy[1]

[1]Dept of Mechanical Engineering, University of Melbourne, Parkville, Victoria 3010

[2]Dept of Surgery, University of Melbourne, St. Vincent's Hospital, Fitzroy, Victoria 3065

[3]Department of Orthopaedics, St. Vincent's Hospital, Fitzroy, Victoria, 3065

Submitted to the Journal of Orthopaedic Research

17 December 2019

Word count: Introduction through to Discussion (3860); Abstract (274)

Author Contributions: MGP, PFC and MMD conceptualized and managed the study. MGP and PFC acquired funding for the research. HG, GS and TJY collected the data. HG, GS and MGP analyzed the data and wrote the original draft. All authors read and edited the final submitted manuscript.

Corresponding author:

Marcus G. Pandy, Ph.D.

Department of Mechanical Engineering

The University of Melbourne

Parkville, Victoria 3010, Australia

email: pandym@unimelb.edu.au

Running title: **TKA knee kinematics during walking**

ABSTRACT

Accurate knowledge of knee joint motion is needed to evaluate the effects of implant design on functional performance and component wear. We conducted a randomized controlled trial to measure and compare 6-degree-of-freedom (6-DOF) kinematics and femoral condylar motion of posterior-stabilized (PS), cruciate-retaining (CR) and medial-stabilized (MS) knee implant designs for one cycle of walking. A mobile biplane X-ray imaging system was used to accurately measure 6-DOF tibiofemoral motion as patients implanted with PS (n = 23), CR (n = 25) or MS (n = 26) knees walked over ground at their self-selected speeds. Knee flexion angle (maximum, minimum, and peak-to-peak range) did not differ significantly between the three designs. Relative movements of the femoral and tibial components were generally similar for PS and CR with significant differences observed only for anterior tibial drawer. Knee kinematic profiles measured for MS were appreciably different: external rotation and abduction of the tibia were increased while peak-to-peak anterior drawer was significantly reduced for MS compared to PS and CR. Anterior-posterior drawer and medial-lateral shift of the tibia were strongly coupled to internal-external rotation for MS, as was anterior-posterior translation of the contact center in the lateral compartment. MS exhibited the least amount of paradoxical anterior translation of the femur relative to the tibia during knee flexion. The joint center of rotation in the transverse plane was located in the lateral compartment for PS and CR and in the medial compartment for MS. Substantial differences were evident in 6-DOF knee kinematics between the healthy knee and all three prosthetic designs. Overall, knee kinematic profiles observed for MS resemble those of the healthy joint more closely than PS and CR.

INTRODUCTION

Total knee arthroplasty (TKA) has proven to be a highly successful treatment for end-stage knee osteoarthritis with excellent longevity and survivorship[1,2]. However, recent studies evaluating patient reported outcomes reveal that nearly one in five patients undergoing TKA surgery remain dissatisfied[3,4], with joint pain and reduced range of motion often cited as serious concerns. Accurate knowledge of knee joint motion during daily activities such as walking would provide much needed insight into the biomechanical mechanisms underlying poor patient outcomes subsequent to TKA surgery.

The most popular total knee prostheses are the conventional cruciate-retaining (CR) and posterior-stabilized (PS) designs[5]. These low-conforming implants have similar component geometries and differ mainly in respect to the cam-and-post mechanism introduced to compensate for resection of the posterior cruciate ligament in the PS design. Anterior translation of the femur relative to the tibia with knee flexion (termed 'paradoxical' motion), reduced posterior translation of the femur with knee flexion (referred to as 'roll-back'), and reversed axial rotation of the knee (i.e., internal rotation of the femur with knee flexion) are often observed in studies evaluating the performance of CR and PS designs[6,7]. These kinematic abnormalities may adversely affect an implant's function and longevity; for example, paradoxical anterior

translation of the femur may potentially reduce the moment arm of the quadriceps muscles and compromise the effectiveness of the knee-extensor mechanism.

Medial stabilized (MS) prostheses are characterised as high-conforming implants and represent a recent innovation in TKA design. The MS prosthesis was developed to more closely approximate motion and stability of the normal knee,[1,8,9] and is comprised of a spherical medial femoral component together with a tibial bearing that is highly conforming on the medial side and relatively flat on the lateral side. Its design is founded on the premise that the femur pivots about the medial compartment in the healthy knee, conferring greater anterior-posterior translation of the lateral femoral condyle during flexion[1,8,10,11]. Recent studies using single-plane X-ray fluoroscopy have shown that MS knees demonstrate minimal anterior-posterior translation of the medial femoral condyle, consistent roll-back of the lateral femoral condyle, and little or no paradoxical anterior translation of the femur with knee flexion[12,13].

Whilst changes in knee kinematics subsequent to TKA surgery have been reported for a wide range of tasks, including chair rise[14,15], stair ambulation[12,15], deep knee bend[16,17], forward lunge[18] and walking[19,20], no study to our knowledge has compared six-degree-of-freedom (6-DOF) knee joint motion for daily activities such as walking across different TKA designs. The aim of the present study was to conduct a randomized controlled trial to measure and compare 6-DOF knee kinematics and femoral condylar motion for PS, CR and MS prostheses as individuals walked at their self-selected speeds over ground. A mobile biplane X-ray imaging system quantified 6-DOF knee joint motion for one full cycle of gait. Significant differences between MS and the PS and CR prostheses were expected given the contrasting features in geometrical design.

MATERIALS AND METHODS

Design: Randomized controlled trial (RCT)

Level of Evidence: I

A prospective, blinded, randomized controlled trial was performed to compare 6-DOF knee joint kinematics for PS (GMK Primary Posterior-stabilized), CR (GMK Primary Cruciate-retaining), and MS (GMK Sphere) total knee arthroplasties sourced from a single manufacturer (Medacta International, Switzerland). The study was approved by the Human Research Ethics Committees of the University of Melbourne and St.

Vincent's Hospital, and is registered at the Australian and New Zealand Clinical Trial Registry (ANZCTR, identifier: ACTRN12613001278729).

Patients referred to St. Vincent's Hospital Melbourne with a clinical and radiographic diagnosis of knee osteoarthritis who were 50 to 80 years of age and on the waiting list for primary total knee arthroplasty were eligible to participate. Exclusion criteria included a BMI > 36.0 kg/m^2 and the inability to ambulate independently. Each patient gave informed consent prior to recruitment. A PS, CR or MS knee was randomly assigned to each patient who was blinded to the type of implant received. The surgical procedure and instrumentation used for all three TKA designs were identical except that the posterior cruciate ligament was left intact in the CR knees and resected when implanting the PS and MS knees. All three TKA designs required resection of the anterior cruciate ligament. Tibial component geometry was identical for the three designs. The geometries of the femoral components and tibial bearings were identical for PS and CR, except for the cam-and-post mechanism present only in the PS design. The tibial bearings for PS and CR were symmetric in the sagittal plane and comprised two shallow concave plateaux. The MS knee featured a femoral component with a spherical medial condyle and a tibial bearing comprised of a highly conforming medial plateau and a nonconforming lateral plateau. The lateral plateau was flat and parallel to the tibial tray with no upslope in the anterior-posterior direction. Thus, unlike the PS and CR tibial bearings, the MS tibial bearing did not restrict internal-external rotation of the femur on the tibia. Details of the inclusion and exclusion criteria, participant recruitment, randomization and surgical procedure are reported elsewhere[21]. Seventy-four patients were tested 6 months after surgery with a roughly equal number of patients receiving each TKA design (Fig. 1, Table 1).

Gait Experiments

Each patient wore a lead vest, shorts and a pair of sandals during testing. Forty-five retro-reflective markers were attached on the surface of the skin at predetermined locations on the upper and lower limbs[22]. The patient then practiced walking over ground at their self-selected speed, first without and then with a Mobile Biplane X-ray (MoBiX) imaging system tracking the knee prosthesis (Fig. 2).[23] Once the patient was comfortable performing the task, full-body 3D motion, ground reaction forces, and X-ray images of the prosthesis were recorded simultaneously for one gait cycle. Data were also recorded as each patient stood with their feet apart at shoulder width and the arms abducted.

Full-body 3D motion data were recorded using a 9-camera motion capture system (VICON Motion Systems, Ltd, Oxford, UK) sampling at 120 Hz. Ground reaction forces were measured using two portable strain-gauged force plates (AMTI Accugait, Watertown, MA) mounted flush with a 4.8 m long walkway and sampling at 1080 Hz. Biplane X-ray images (1024×1024 pixels) of the prosthesis were acquired at 200 frames/sec with an exposure time of 1/200 sec (Fig. 2). Maximum RMS errors for translations and rotations of a knee prosthesis measured during a simulated gait cycle using the MoBiX imaging system were previously reported to be 0.33 mm and 0.65°, respectively[23].

Data Analysis

6-DOF knee kinematics for one gait cycle was described as the motion of the tibia with respect to the femur (Fig. 3). The rotations and translations of the tibia relative to the femur were calculated at 201 equally-spaced time points using the biplane X-ray images together with 3D models of the femoral and tibial components provided by the implant manufacturer. Details of the methods used to calculate knee kinematics, including calibration, image processing and pose estimation, are given by Guan et al.[23]. Gait events were identified using the measured ground reaction forces and trajectories of the heel markers[24].

We also measured the movements of the femoral condyles and corresponding centers of tibiofemoral joint contact as well as the location of the center of rotation of the knee in the transverse plane, all of which were described in the tibial reference frame (Fig. 3). Femoral condylar motion was described as the translations of the centers of the femoral condyles, which were located at the intersections between the femoral X-axis and each mid-condylar sagittal plane (parallel to the femoral Y-Z plane in Fig. 3). The contact centers in the medial and lateral compartments of the tibiofemoral joint were found by calculating the minimum distance between each femoral condyle and the tibial tray at each time point[24]. The center of rotation of the knee in the transverse plane was found by projecting the femoral X-axis onto the tibial X-Y plane at each time point and then finding the intersection of these lines in a least-squares sense[25,26].

Spline functions were fit to the mean 6-DOF kinematic parameters measured for each TKA group to assess the degree to which each DOF is coupled to flexion-extension and internal-external rotation of the knee[26]. The coefficient of determination (r^2) and Root Mean Square Error (RMSE) derived from these calculations indicate how strongly any given rotation or translation of the tibia relative to the femur is coupled to flexion-extension and internal-external rotation. An r^2 value of 1.0 and an RMSE value of 0.0 would indicate perfect coupling.

Measured translations of the tibia relative to the femur, motion of the femoral condylar centers, motion of the tibiofemoral contact centers, and the location of the center of rotation of the knee in the transverse plane were all normalized using the ratio of the anterior-posterior length of an individual patient's femoral component to the mean anterior-posterior length of the femoral component calculated for all 74 patients. Data recorded for the three groups were compared by calculating the maximum, minimum, peak-to-peak (maximum - minimum), and mean value of each outcome variable over one gait cycle. A one-way analysis of variance (ANOVA) was used to identify the outcome variables which were significantly different ($p < 0.05$) between the three implant designs. Student t-tests were then performed on those outcome variables to determine whether there was a significant difference between each paired combination of the three designs. A conservative threshold of significance was set at $p < 0.017$ for all tests. This p value was determined by applying a Bonferroni correction using an initial significance threshold of $p < 0.05$ and three pairwise comparisons per dependent variable.

RESULTS

Mean walking speed was not statistically different between the three groups (0.86 ± 0.14 m/s, 0.82 ± 0.17 m/s and 0.87 ± 0.14 m/s for PS, CR and MS, respectively, all $p > 0.25$). Trajectories of lower-limb joint kinematics and kinetics computed from full-body video motion capture and force plate measurements were grossly similar across the three groups, with a few significant differences noted in the measured ankle and subtalar joint angles, mediolateral ground reaction force, and hip and knee flexion-extension moments (see Supplementary Material). 6-DOF rotations and translations of the tibia relative to the femur measured from mobile X-ray imaging were significantly different for MS compared to PS and CR (Fig. 4, Table 2).

Six-degree-of-freedom knee kinematics

There was no significant difference in knee flexion angle between the three groups (Fig. 4, Table 2). Peak-to-peak anterior-posterior translation for PS (9.9 mm) was significantly greater than that for CR (7.8 mm), which in turn was significantly greater than that for MS (4.4 mm) (Table 2, all $p \leq 0.004$). Maximum external tibial rotation was 3.5° greater for MS than PS (Table 2, $p = 0.013$). Although MS was more abducted than CR ($p = 0.012$) and less distracted than both PS and CR ($p \leq 0.01$), these differences were relatively small (Table 2). For standing, joint distraction was the only kinematic parameter that differed significantly among the three TKA designs, with PS being 0.5 mm more distracted than MS ($p<0.001$). MS was also more externally rotated (by ~3.2°) than PS and CR during standing, although this difference did not reach statistical significance (Fig. 4, Table 2, $p<0.033$).

Joint distraction was strongly coupled to knee flexion for all three designs (Fig. 5A, $r^2 \geq 0.83$). Anterior drawer, lateral shift and abduction of the tibia relative to the femur were each moderately coupled to the flexion angle for all three designs (Fig. 5A, $r^2 > 0.42$). Anterior drawer and lateral shift were both strongly coupled to external rotation for MS only ($r^2 > 0.79$) (Fig. 5B).

Motion of the femoral condyles and tibiofemoral joint contact centers

The femoral condyles translated predominantly in the anterior-posterior direction relative to the tibia for all three designs (Fig. 6A and B). Peak-to-peak anterior-posterior translation of the medial condyle for MS (3.0 mm) was significantly less than that for CR (8.2 mm), which in turn was significantly less than that for PS (11.1 mm) (Table 3, all $p \leq 0.001$). The center of the medial condyle for MS was located ~2 mm more laterally compared to PS and CR in both standing and walking (all $p < 0.001$). Anterior-posterior translation of the lateral condyle was strongly coupled to external rotation of the tibia for MS only ($r^2 = 0.93$) (Fig. 6C).

Consistent with the movements of the femoral condyles, peak-to-peak anterior-posterior translation of the medial contact center over one complete gait cycle for MS (3.4 mm) was significantly less than that for CR (7.1 mm), which in turn was significantly less than that for PS (9.9 mm) (Fig. 7 and Table 4, all $p < 0.001$). There was no significant difference in peak-to-peak anterior-posterior translation of the

lateral contact center between the three groups (Table 4). Anterior-posterior translation of the lateral contact center was strongly coupled to external rotation of the tibia for MS only ($r^2 = 0.84$) (Fig. 7C).

Transverse center of rotation of the knee

For MS, the center of rotation of the knee in the transverse plane was located 19.4 mm and 21.8 mm medial to the tibial origin during stance and swing, respectively (Fig. 8). By comparison, the centers of rotation for PS and CR remained in the lateral compartment throughout the gait cycle. For PS the center of rotation was located 6.4 mm and 12.2 mm lateral to the tibial origin during stance and swing, respectively, whereas for CR the center of rotation was 16.2 mm and 15.2 mm lateral to the tibial origin during stance and swing.

DISCUSSION

We used a unique mobile biplane X-ray imaging system to accurately measure 6-DOF knee kinematics and femoral condylar motion during walking in patients implanted with PS, CR and MS knees. Knee flexion was the only kinematic variable that did not differ significantly between the three TKA designs. Overall, relative movements of the femoral and tibial components were similar for PS and CR with significant differences noted only for anterior tibial drawer. Translations of the femoral condyles and tibiofemoral joint contact centers were also similar for these two designs. In contrast, the profiles of knee joint motion for MS were appreciably different: MS was more externally rotated than PS and more abducted than CR while peak-to-peak anterior drawer for MS was approximately one-half of that measured for the other two designs. Anterior tibial drawer and lateral tibial shift were strongly coupled to external rotation of the tibia for MS, as was anterior-posterior translation of the lateral femoral condyle. The center of rotation of the knee in the transverse plane was located in the lateral compartment for PS and CR and in the medial compartment for MS.

Relatively few differences were found in the kinematic and kinetic profiles calculated from video motion capture and force plate measurements across all three groups, yet the 6-DOF movements of the femoral and tibial components measured for MS were significantly different from those obtained for PS and CR. Some of the differences in the measured 6-DOF knee kinematic profiles may be explained by (a) the relatively small but nonetheless significant differences noted in ankle joint motion and hip and knee flexion-extension moments in the sagittal plane (Tables S1 and S3 in Supplementary Material); and/or (b) differences in the frontal- and transverse-plane moments exerted about the knee, which were not computed here. Future work should aim to reconcile differences in 6-DOF knee kinematics measured for various implant designs with accurate estimates of non-sagittal-plane knee joint moments.

Differences in 6-DOF knee kinematics measured between MS and the PS and CR prostheses reflect the highly congruent medial articulation characterizing the MS design, which limited translations of the medial femoral condyle and coupled translations of the lateral femoral condyle to internal-external rotation of the tibia. Anterior tibial translation and lateral tibial shift were also strongly coupled to external

rotation of the tibia for MS, implying that this design behaves as a two-degree-of-freedom joint with the femur pivoting about the medial femoral condyle during flexion-extension movements of the knee. Differences in joint motion between PS and CR were comparatively small and suggest that the cam-and-post mechanism compensated effectively for the resected posterior cruciate ligament in the PS design. It is also possible, however, that the posterior cruciate ligament remained slack in the CR prosthesis, and that differences in anterior-posterior translation between PS and CR were due to the cam-and-post engaging only at high knee flexion angles.

Recent data obtained for normal walking[26] reveal substantial differences in 6-DOF kinematics between the healthy knee and all three TKA designs, particularly with respect to knee flexion, anterior tibial drawer, lateral tibial shift, external tibial rotation, femoral roll-back, and screw-home motion of the knee (i.e., external rotation of the tibia relative to the femur in terminal extension[27]) (Figs 9, 10). Consistent with previous studies[28,29], peak knee flexion angles during stance and swing for the TKA knees are, respectively, 5° and 14° less than that measured for the healthy joint (Fig. 9). The tibia is also more posteriorly translated and medial-lateral shift noticeably reduced in the TKA knees compared to the healthy joint. Abduction and joint distraction remain relatively constant for the duration of the gait cycle in the healthy knee and all three prosthetic designs.

Femoral roll-back with knee flexion, medial pivoting in the transverse plane throughout the gait cycle, and screw-home motion during late swing are all characteristic features of normal walking[26]. The PS and CR designs displayed the opposite behavior: anterior translation of the femur relative to the tibia with knee flexion during late stance, lateral pivoting in the transverse plane throughout the gait cycle (Fig. 8), and a loss of screw-home motion during terminal swing manifested as reversed axial rotation (i.e., internal rotation) of the tibia with knee extension (Fig. 5A). Previous studies also have reported a transverse center of rotation located in the lateral compartment for CR,[30] paradoxical anterior translation of the femur for CR[30–32], reduced roll-back of the femur in CR and PS[33], and a loss of screw home motion in PS[34]. Whilst the behavior of MS was similar to that of PS and CR with respect to anterior translation of the femur in terminal stance and a loss of screw-home motion in terminal swing, the center of rotation in the transverse plane was clearly in the medial compartment, similar to that reported for the healthy knee in normal walking.

All three TKA designs showed a limited amount of anterior translation of the femur relative to the tibia as the knee flexed immediately after contralateral heel-strike during late stance. Many investigators have observed this behavior in various TKA designs, referring to it as ‘paradoxical’ motion because the femur is thought to translate posteriorly with flexion in the healthy knee[7,13,35]. However, recent data reported by Gray et al.[26] for the healthy knee show that the femur does indeed translate anteriorly with flexion during late stance, albeit by a smaller amount than that observed in the TKA knees, particularly for the PS and CR designs. Nonetheless, anterior translation of the femur during late stance may not be a major concern functionally, as the ground reaction force, and hence the load transmitted by the knee joint, are rapidly decreasing at this time. Whilst a more anterior position of the femur

may potentially compromise the effectiveness of the knee-extensor mechanism, during late stance the quadriceps muscles are involved in preparing the limb for swing rather than in stabilizing the body under its own weight, as is necessary during weight acceptance in early stance.

The difference in knee flexion angle between the healthy and implanted knees is likely explained by the lower walking speed adopted by the TKA patients. The younger healthy subjects (30.5±6.2 years old) tested by Gray et al.[26] walked at a mean speed of 1.28 m/s compared to 0.85 m/s measured for the TKA patients here. Previous studies have shown that peak knee flexion angles during stance and swing increase with walking speed[36–38]. The differences observed in secondary joint motions between the TKA and healthy knees may be due to differences in the shapes of the articulating surfaces of the TKA components as well as changes to the geometry of the cruciate ligaments introduced at the time of surgery. Ng et al.[39] found that anterior-posterior translations of the medial and lateral femoral condyles were altered subsequent to anterior-cruciate-ligament (ACL) injury, resulting in a loss of screw-home motion. Others have found that ACL-retaining implants function better than ACL-resecting designs in relation to internal-external rotation.[7] All TKA knees in the present study required ACL resection, which may explain the altered condylar translation and absence of screw-home motion observed (Fig. 10).

During standing, the TKA knees were up to 8° more flexed and up to 9° more internally rotated than the healthy knee (Fig. 9). The tibial components in the prostheses were also translated more anteriorly and medially than the tibia in the healthy joint (Fig. 9). Increased external rotation of the tibia during standing in the healthy knee is clearly evidenced by the difference in anterior positions of the condylar centers in the medial and lateral compartments compared to that observed for all three TKA designs (Fig. 10A). These differences in joint configuration for standing are likely to reflect the differences in joint geometry between the healthy knee and the prostheses as well as changes to the tensioning of the collateral ligaments introduced during surgery. Similarly, differences in knee kinematics measured for standing between MS and the PS and CR designs (i.e., MS exhibited increased external tibial rotation and reduced anterior tibial drawer) are presumably the result of a highly congruent medial articulation in the MS design.

One potential limitation of the present study is that the TKA patients were tested only 6 months after surgery, which may explain why mean walking speed (~0.85 m/s) was at the lower end of the range of self-selected walking speeds reported by others (0.8-1.1 m/s)[40]. Whilst there is some evidence to suggest that gait biomechanics may take longer than 6 months to stabilize[29,41], post-surgery recovery time was similar across all three groups. It is possible that some of the differences observed between the TKA knees and the healthy joint may diminish over time. For example, knee flexion excursion during the weight acceptance phase of the gait cycle was found to be 4.4° less for TKA patients at 3 months post-surgery compared to age-matched controls, but no different at 2-3 years post-surgery[29]. Another limitation of our results is that they apply only to walking on level ground. Future work should focus on measuring 6-

DOF knee kinematics for different TKA designs in other activities of daily living such as rising from a chair and walking up and down stairs.

We quantitatively compared 6-DOF knee kinematics across different TKA designs for both the stance and swing phases of the walking cycle. Consistent with the contrasting features in geometrical design, knee kinematic profiles for MS were significantly different from those observed for the PS and CR designs. Peak-to-peak anterior tibial drawer was significantly less for MS than for CR and PS, external tibial rotation was significantly greater for MS than PS and MS was significantly more abducted than CR. Significant differences were evident in 6-DOF kinematics between the healthy knee and all three TKA designs. The kinematic profiles for MS resembled those of the healthy joint more closely than PS and CR.

ACKNOWLEDGEMENTS

This study was funded by Medacta International, Frauenfeld, Switzerland.

REFERENCES

1. Macheras GA, Galanakos SP, Lepetsos P, et al. 2017. A long term clinical outcome of the Medial Pivot Knee Arthroplasty System. Knee 24:447–453.

2. Argenson JN, Boisgard S, Parratte S, et al. 2013. Survival analysis of total knee arthroplasty at a minimum 10 years' follow-up: A multicenter French nationwide study including 846 cases. Orthop Traumatol Surg Res 99:385–390.

3. Bourne RB, Chesworth BM, Davis AM, et al. 2010. Patient satisfaction after total knee arthroplasty: Who is satisfied and who is not? Clin Orthop Relat Res 468:57–63.

4. Dunbar MJ, Richardson G, Robertsson O. 2013. I can't get no satisfaction after my total knee replacement: rhymes and reasons. Bone Joint J 95-B:148–152.

5. Pritchett JW. 2011. Patients Prefer A Bicruciate-Retaining or the Medial Pivot Total Knee Prosthesis. J Arthroplasty 26:224–228.

6. Dennis DA, Komistek RD, Mahfouz MR, et al. 2003. Conventry Award Paper: Multicenter Determination of In Vivo Kinematics After Total Knee Arthroplasty. Clin Orthop Relat Res 416:37–57.

7. Dennis DA, Komistek RD, Mahfouz MR, et al. 2004. A multicenter analysis of axial femorotibial rotation after total knee arthroplasty. Clin Orthop Relat Res :180–189.

8. Schmidt R, Komistek RD, Blaha JD, et al. 2003. Fluoroscopic analyses of cruciate-retaining and medial pivot knee implants. Clin Orthop Relat Res 410:139–147.

9. Fitch DA, Sedacki K, Yang Y. 2014. Mid- to long-term outcomes of a medial-

pivot system for primary total knee replacement: a systematic review and meta-analysis. Bone Jt Res 3:297–304.

10. Hollister AM, Jatana S, Singh AK, et al. 1993. The axes of rotation of the knee. Clin Orthop Relat Res 290:259–268.

11. Churchill DL, Incavo SJ, Johnson CC, Beynnon BD. 1998. The transepicondylar axis approximates the optimal flexion axis of the knee. Clin Orthop Relat Res 356:111–118.

12. Scott G, Imam MA, Eifert A, et al. 2016. Can a total knee arthroplasty be both rotationally unconstrained and anteroposteriorly stabilised?: A pulsed fluoroscopic investigation. Bone Jt Res 5:80–86.

13. Schütz P, Taylor WR, Postolka B, et al. 2019. Kinematic Evaluation of the GMK Sphere Implant during Gait Activities: A Dynamic Videofluoroscopy Study. J Orthop Res:jor.24416.

14. Fantozzi S, Catani F, Ensini A, et al. 2006. Femoral rollback of cruciate-retaining and posterior-stabilized total knee replacements: In vivo fluoroscopic analysis during activities of daily living. J Orthop Res 24:2222–2229.

15. Murakami K, Hamai S, Okazaki K, et al. 2018. Knee kinematics in bi-cruciate stabilized total knee arthroplasty during squatting and stair-climbing activities. J Orthop 15:650–654.

16. Ranawat CS, Komistek RD, Rodriguez JA, et al. 2004. In vivo kinematics for fixed and mobile-bearing posterior stabilized knee prostheses. Clin Orthop Relat Res 80222:184–190.

17. Bertin KC, Komistek RD, Dennis DA, et al. 2002. In vivo determination of posterior femoral rollback for subjects having a NexGen posterior cruciate-retaining total knee arthroplasty.17:1040–1048.

18. Hanson GR, Suggs JF, Freiberg AA, et al. 2006. Investigation of in vivo 6DOF total knee arthoplasty kinematics using a dual orthogonal fluoroscopic system. J Orthop Res 24:974–981.

19. Taylor WR, Schütz P, Bergmann G, et al. 2017. A comprehensive assessment of the musculoskeletal system: The CAMS-Knee data set. J Biomech 65:32–39.

20. DesJardins JD, Banks SA, Benson LC, et al. 2007. A direct comparison of patient and force-controlled simulator total knee replacement kinematics. J Biomech 40:3458–3466.

21. Dowsey MM, Pandy M, Young TJ, et al. 2018. A blinded, three-arm randomised trial assessing joint function and measuring three-dimensional knee joint kinematics in individuals six months after a total knee joint replacement; comparing a medially stabilised design, to standard fixed bearing conventi. Int J

Clin Trials; Vol 5, No 1 January-March 2018 5:37–45.

22. Lai A, Lichtwark GA, Schache AG, et al. 2015. In-vivo behavior of the human soleus muscle with increasing walking and running speeds. J Appl Physiol 118:1266–1275.

23. Guan S, Gray HA, Keynejad F, Pandy MG. 2016. Mobile biplane X-ray imaging system for measuring 3D dynamic joint motion during overground gait. Med Imaging, IEEE Trans 35:326–336.

24. Guan S, Gray HA, Schache AG, et al. 2017. In vivo six-degree-of-freedom knee-joint kinematics in overground and treadmill walking following total knee arthroplasty. J Orthop Res 35.

25. Koo S, Andriacchi TP. 2008. The knee joint center of rotation is predominantly on the lateral side during normal walking. J Biomech 41:1269–1273.

26. Gray HA, Guan S, Thomeer LT, et al. 2019. Three-dimensional motion of the knee-joint complex during normal walking revealed by mobile biplane x-ray imaging. J Orthop Res 37:615–630.

27. Trent PS, Walker PS, Wolf B. 1976. Ligament length patterns, strength, and rotational axes of the knee joint. Clin Orthop Relat Res 117:263–270.

28. Andriacchi TP, Galante JO, Fermier RW. 1982. The influence of total knee-replacement design on walking and stair-climbing. J Bone Joint Surg Am 64:1328–1335.

29. Yoshida Y, Zeni JA, Snyder-Mackler L. 2012. Do patients achieve normal gait patterns 3 years after total knee arthroplasty? Orthop Sport Phys Ther 29:997–1003.

30. Ploegmakers MJM, Ginsel B, Meijerink HJ, et al. 2010. Physical examination and in vivo kinematics in two posterior cruciate ligament retaining total knee arthroplasty designs. Knee 17:204–209.

31. Donadio J, Pelissier A, Boyer P, Massin P. 2015. Control of paradoxical kinematics in posterior cruciate-retaining total knee arthroplasty by increasing posterior femoral offset. Knee Surgery, Sport Traumatol Arthrosc 23:1631–1637.

32. Varadarajan KMM, Zumbrunn T, Rubash HE, et al. 2015. Cruciate retaining implant with biomimetic articular surface to reproduce activity dependent kinematics of the normal knee. J Arthroplasty 30:2149-2153.e2.

33. Varadarajan KM, Harry RE, Johnson T, Li G. 2009. Can in vitro systems capture the characteristic differences between the flexion-extension kinematics of the healthy and TKA knee? Med Eng Phys 31:899–906.

34. Bull AMJ, Kessler O, Alam M, Amis AA. 2008. Changes in knee kinematics

reflect the articular geometry after arthroplasty. Clin Orthop Relat Res 466:2491–2499.

35. Dennis DA, Komistek RD, Mahfouz MR. 2003. In Vivo Fluoroscopic Analysis Of Fixed-Bearing Total Knee Replacements. Clin Orthop Relat Res 410.

36. Arendt-Nielsen L, Sinkjær T, Nielsen J, Kallesøe K. 1991. Electromyographic patterns and knee joint kinematics during walking at various speeds. J Electromyogr Kinesiol 1:89–95.

37. Lim YP, Lin Y-C, Pandy MG. 2017. Effects of step length and step frequency on lower-limb muscle function in human gait. J Biomech 57:1–7.

38. Liu MQ, Anderson FC, Schwartz MH, Delp SL. 2008. Muscle contributions to support and progression over a range of walking speeds. J Biomech 41:3243–52.

39. Ng AWH, Griffith JF, Hung EHY, et al. 2013. Can MRI predict the clinical instability and loss of the screw home phenomenon following ACL tear? Clin Imaging 37:116–123.

40. McClelland JA, Webster KE, Feller JA. 2007. Gait analysis of patients following total knee replacement: a systematic review. Knee 14:253–63.

41. Pua Y-H, Seah FJ-T, Clark RA, et al. 2017. Factors associated with gait speed recovery after total knee arthroplasty: A longitudinal study. Semin Arthritis Rheum 46:544–551.

42. Grood ES, Suntay WJ. 1983. A joint coordinate system for the clinical description of three-dimensional motions: application to the knee. J Biomech Eng 105:136–44.

FIGURES

Fig. 1. Consolidated Standards of Reporting Trials (CONSORT) flow diagram.

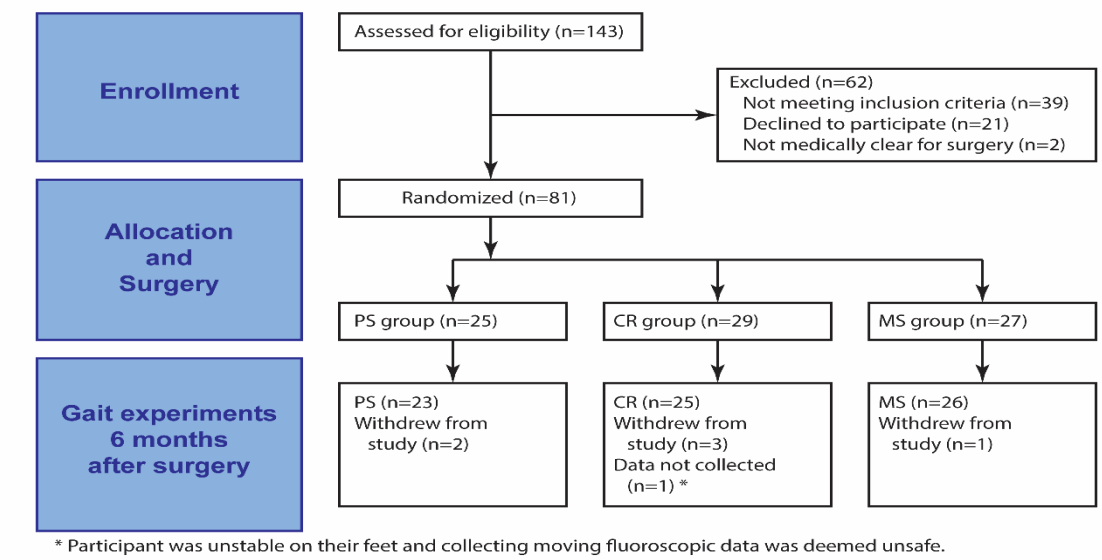

Fig. 2. Mobile Biplane X-ray (MoBiX) imaging system used to measure 6-DOF knee kinematics during walking. A robotic gantry mechanism translated the two X-ray units in the horizontal and vertical directions to track and image the knee joint. A retroreflective marker placed on the lateral side of the test knee (not shown) was imaged by the high-speed Tracking Camera. A real-time computer (Gantry Motion Profiler) processed the marker images and generated velocity commands which controlled the motion of the X-ray units via the servomotors. Two high-speed digital cameras mounted on the two image intensifiers captured biplane X-ray images that were stored on the Operator Workstation. Details of the MoBiX imaging system are given in Guan et al.[23]

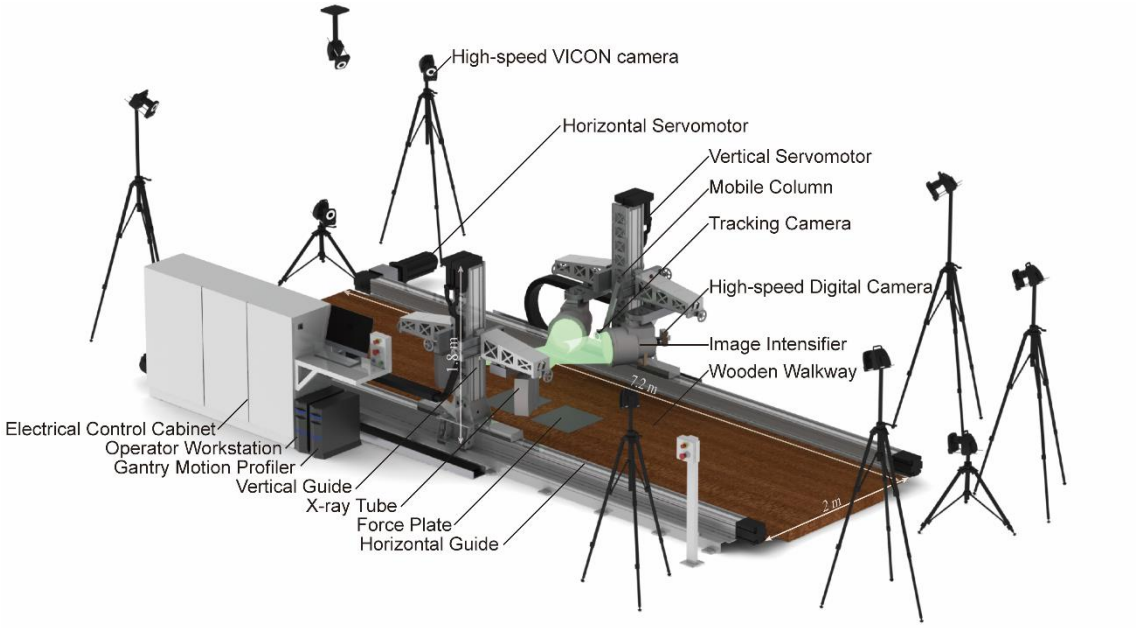

Fig. 3. Six-DOF knee kinematics was described using a joint coordinate system similar to that reported by Grood and Suntay[42]. Coordinate systems defined for the femoral and tibial components are illustrated for a right cruciate-retaining (CR) prosthesis. The femoral coordinate system was constructed by first fitting a cylinder to the posterior and distal parts of both femoral condyles. The axis of the cylinder was defined as the femoral X-axis (X_F) pointing to the right. The femoral origin was defined as the intersection between X_F and the mid-sagittal plane of the femoral component. The Z-axis (Z_F) was defined to be perpendicular to the transverse flat surface of the femoral component and pointed proximally. The Y-axis (Y_F) was mutually perpendicular to X_F and Z_F and pointed

anteriorly. The tibial Z-axis (Z_T) was coincident with the axis of the tibial stem (also perpendicular to the tibial tray) and pointed superiorly. To establish the tibial origin the 3D models of the patient-specific tibial component, tibial bearing, and femoral component were assembled in the neutral configuration with Z_F and Z_T parallel to each other. The tibial origin was located at the intersection between the Z_T axis and the femoral X_F-Y_F plane. The tibial X-axis (X_T) and Y-axis (Y_T) were defined to be parallel to F_X and F_Y, respectively, in the assembled position. To define the translations and rotations of the tibia relative to the femur, X_F and Z_T were used as the body-fixed axes. A floating axis (W) was defined to be instantaneously mutually perpendicular to X_F and Z_T[42]. Flexion (R_1), abduction (R_2) and external rotation (R_3) occurred about the X_F, W and Z_T axes, respectively, while lateral shift (T_1), anterior drawer (T_2) and joint distraction (T_3) were along X_F, W and Z_T, respectively. Arrows in the figure indicate the positive direction of each degree of freedom for the tibia with respect to the femur.

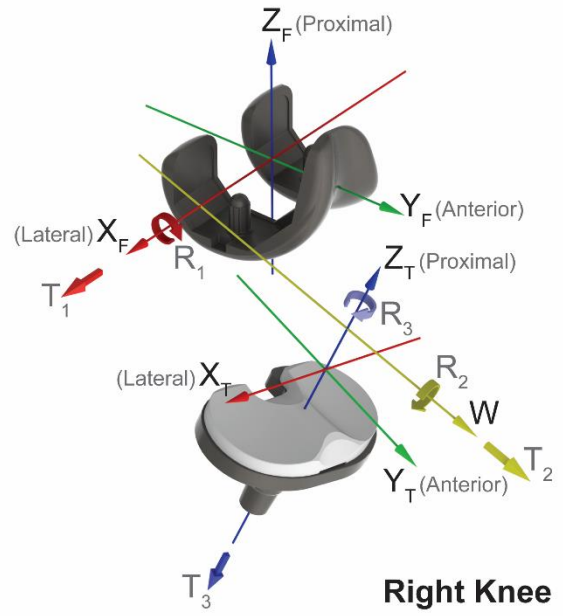

Fig. 4. 6-DOF rotations (top row) and translations (bottom row) of the tibia with respect to the femur measured for standing and one cycle of overground walking. For each patient group, the line and shaded area represent the mean and +1 standard deviation from the mean for walking while the dot and whiskers represent the mean and +1 standard deviation from the mean for standing. The solid lines represent the stance phase while the dashed lines represent the swing phase. The label above each panel indicates the positive direction of the motion displayed. PS, posterior-stabilized; CR, cruciate-retaining; MS, medial-stabilized. Gait events are: HS, heel-strike; TO, toe-off; CHS, contralateral heel-strike; CTO, contralateral toe-off.

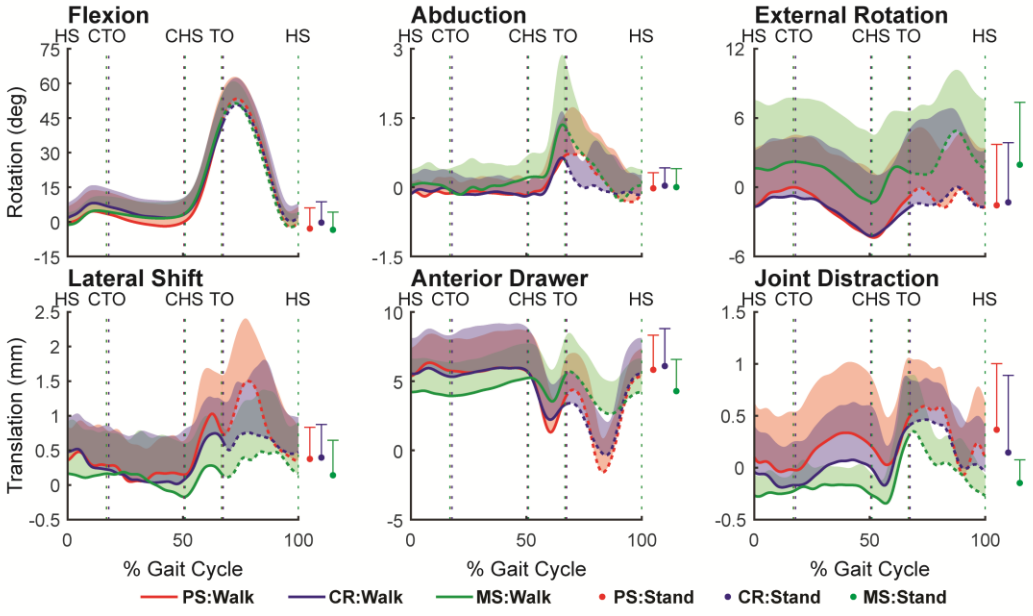

Fig. 5. (A) 6-DOF rotations (top row) and translations (bottom row) of the tibia relative to the femur plotted against the knee flexion angle for standing and one cycle of overground walking. Data shown are the mean for each patient group. (B) 6-DOF rotations (top row) and translations (bottom row) of the tibia relative to the femur plotted against the external rotation angle of the knee for walking and standing. Data shown are the mean for each patient group. The solid lines represent the stance phase while the dashed lines represent the swing phase. The coefficients of determination (r^2) and root mean square error (RMSE) quantify the degree of coupling between the parameters plotted in each panel. RMSE values are in degrees for joint angles and in mm for joint translations. PS, posterior-stabilized; CR, cruciate-retaining; MS, medial-stabilized.

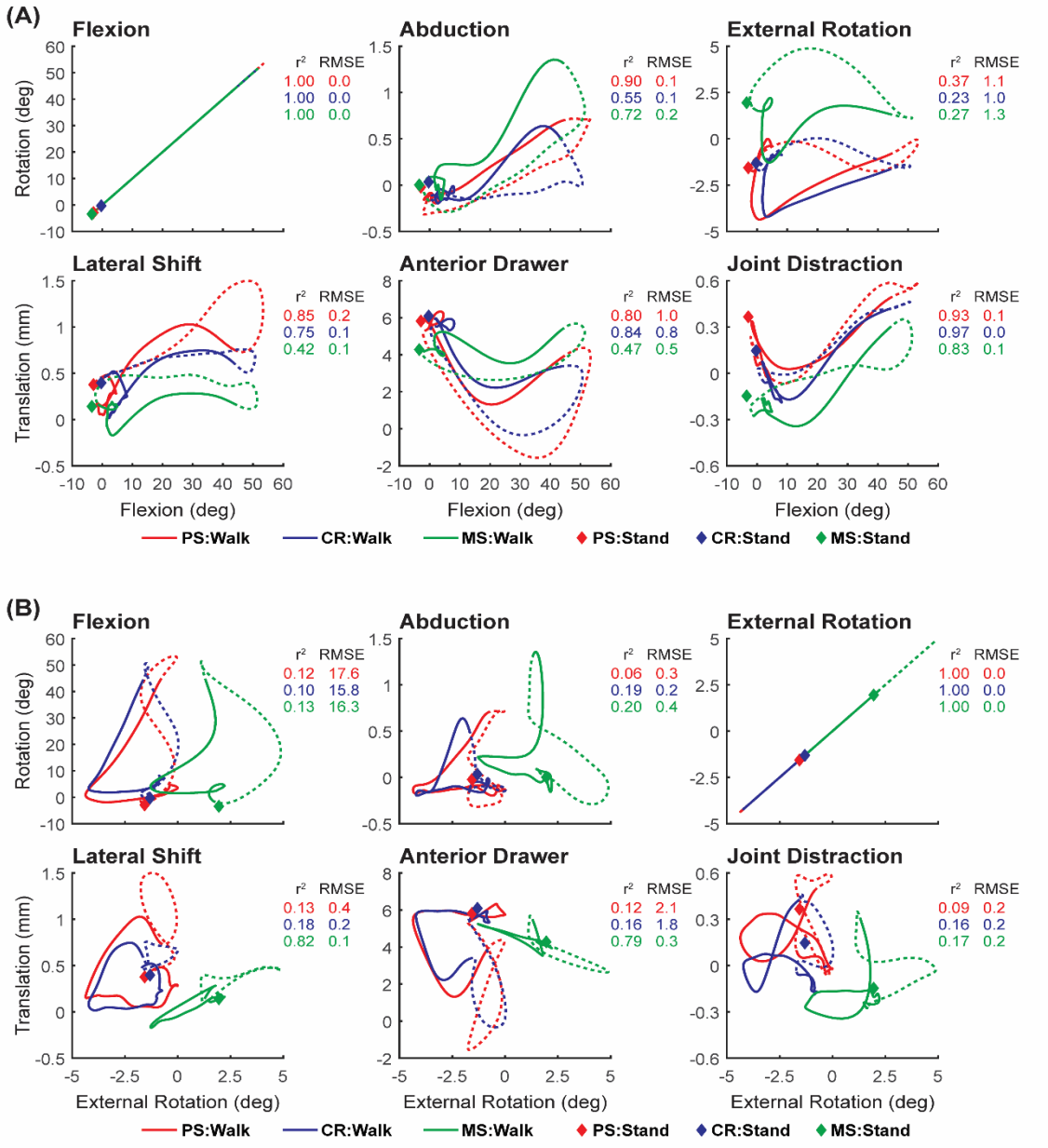

Fig. 6. Motion of the femoral condylar centers relative to the tibial bearing for standing and one cycle of overground walking. Red, blue and green represent the three patient groups: PS, posterior-stabilized; CR, cruciate-retaining; and MS, medial-stabilized. (A) Locations of the medial and lateral femoral condylar centers projected onto the tibial bearing. The insets show magnified views of the motion trajectories. (B) Anterior-posterior translations (top row) and medial-lateral translations (bottom row) of the femoral condylar centers plotted against percentage of the gait cycle. For each group, the line and shaded area represent the mean and +1 standard deviation from the mean for walking; the dot and whiskers represent the mean and +1 standard deviation from the mean for standing. (C) Anterior-posterior translations of the femoral condylar centers plotted against both the knee flexion angle (top row) and external rotation of the tibia (bottom row). The coefficients of determination (r^2) and root mean square error (RMSE in mm) quantify the degree of coupling between the parameters plotted in each panel. Only mean data are shown in (C). Solid lines represent the stance phase and dashed lines represent the swing phase. HS, heel-strike; TO, toe-off; CHS, contralateral heel-strike; CTO, contralateral toe-off.

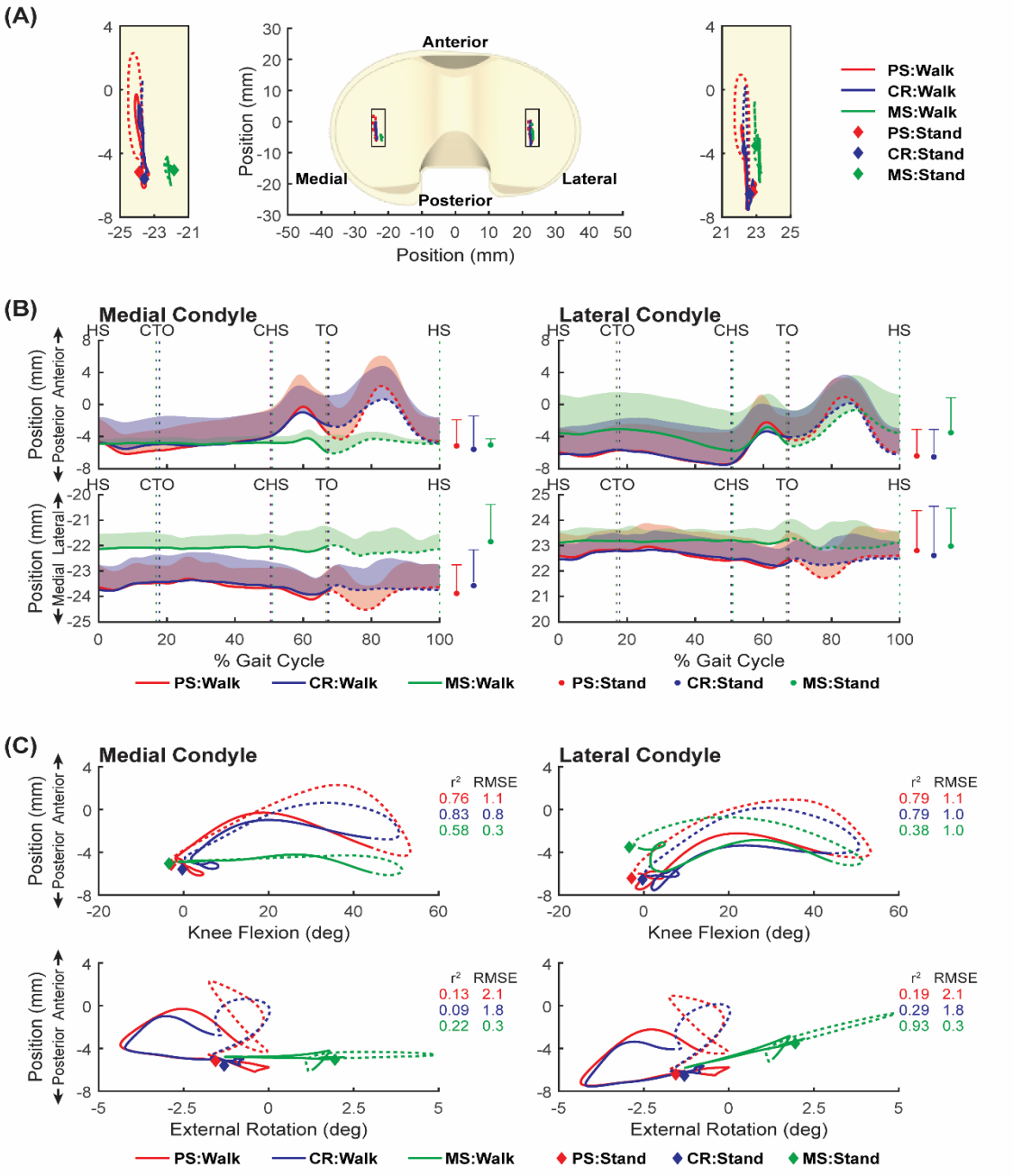

Fig. 7. Locations of the tibiofemoral contact centers measured for standing and one cycle of overground walking. (A) Contact centers on the tibial bearing in the medial and lateral compartments of the tibiofemoral joint. The insets show magnified views of the trajectories of joint contact. (B) Anterior-posterior translations (top row) and medial-lateral translations (bottom row) of the contact centers on the medial and lateral plateaux of the tibial bearing plotted against the percentage of the gait cycle. For each group, the line and shaded area represent the mean and +1 standard deviation from the mean for walking while the dot and whiskers represent the mean and +1 standard deviation from the mean for standing. (C) Anterior-posterior translations of the contact centers on the medial and lateral plateaux of the tibial bearing plotted against both the knee flexion angle (top row) and external rotation of the tibia (bottom row). The coefficients of determination (r^2) and root mean square error (RMSE in mm) quantify the degree of coupling between the parameters plotted in each panel. Only mean data are shown in (C). Solid lines represent the stance phase and dashed lines represent the swing phase. HS, heel-strike; TO, toe-off; CHS, contralateral heel-strike; CTO, contralateral toe-off.

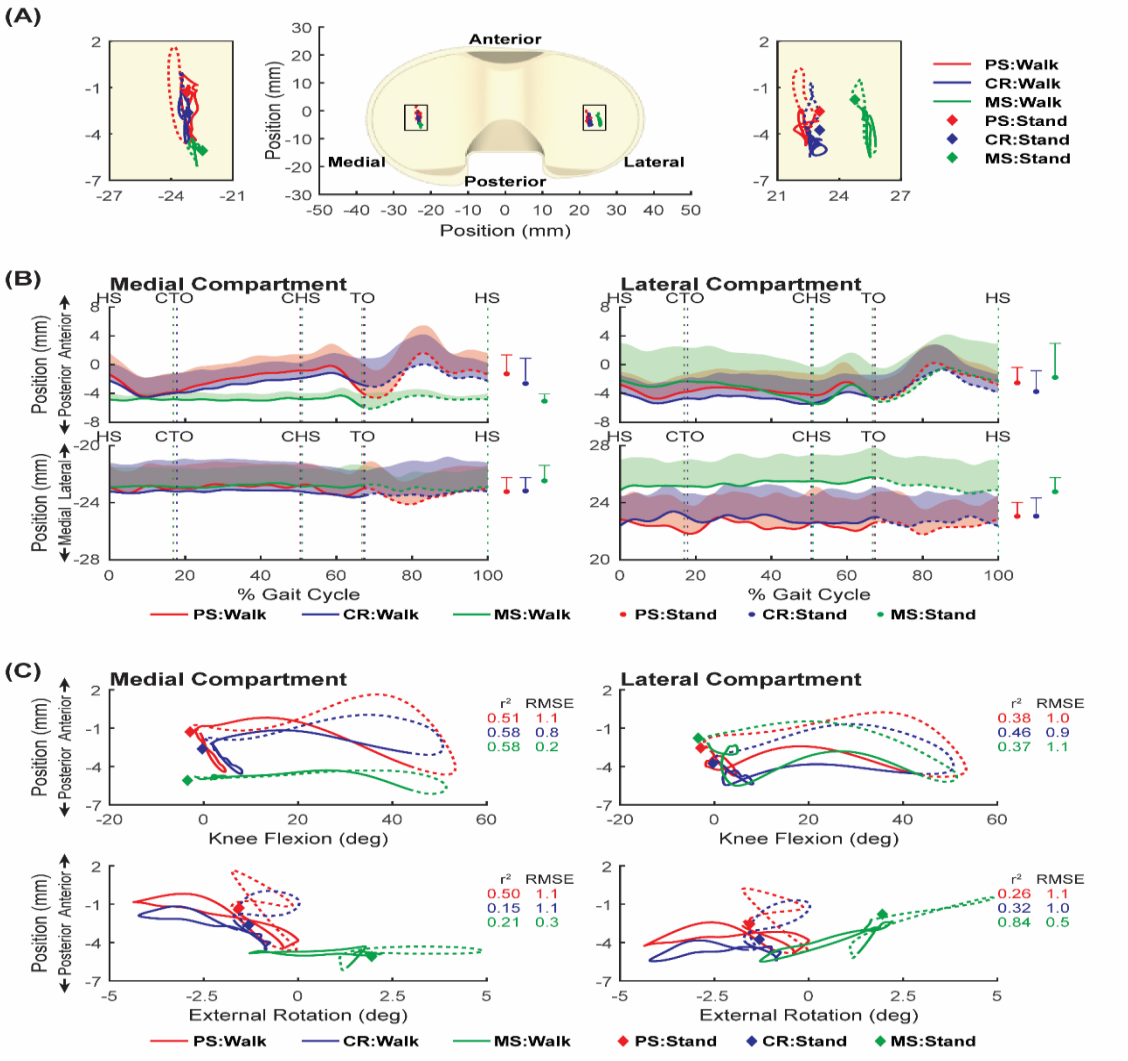

Fig. 8. Location of the knee center of rotation in the transverse plane of the tibia for one gait cycle (top); for the stance phase only (middle); and for the swing phase only (bottom). Red, blue and green represent the three patient groups: PS, posterior-stabilized; CR, cruciate-retaining; and MS, medial-stabilized. The circles represent the mean center of rotation calculated for each TKA design while the error bars represent ±1 standard deviation from the mean.

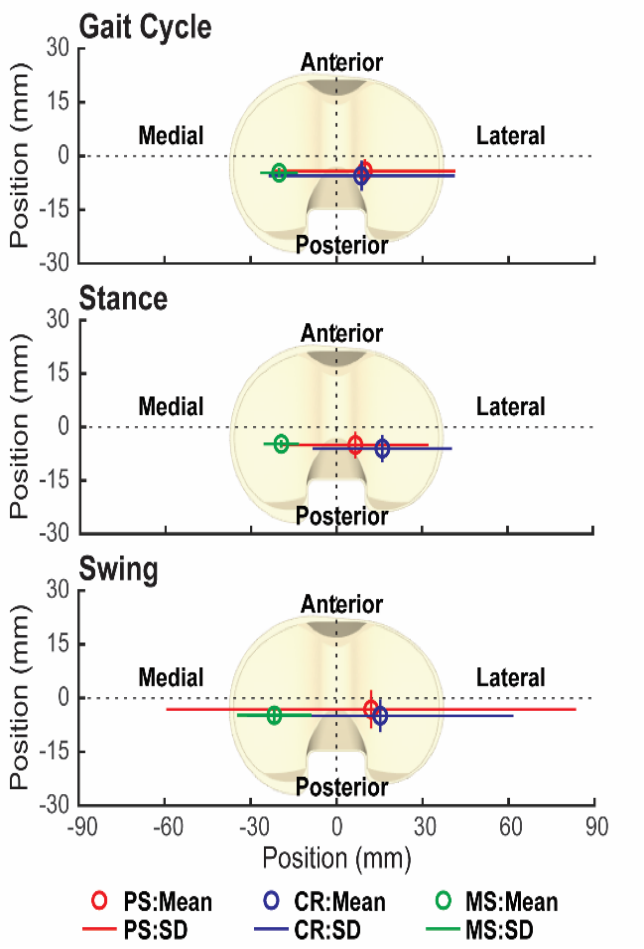

Fig. 9. 6-DOF rotations and translations of the tibia with respect to the femur measured for standing and one cycle of overground walking for the prostheses compared to results previously reported by Gray et al.[26] for the healthy knee. Only mean data are shown for the prostheses: PS, posterior-stabilized; CR, cruciate-retaining; and MS, medial-stabilized. The black solid lines represent the mean values measured for the healthy knee while the grey shaded areas represent ±1 standard deviation from the mean. Each dot and whisker on the far right-side of each panel represent the mean and ±1 standard deviation from the mean for standing for the prostheses and healthy knee. The healthy knee data were re-calculated using a coordinate system similar to that adopted for the prostheses. Solid lines represent the stance phase and dashed lines represent the swing phase. HS, heel-strike; TO, toe-off; CHS, contralateral heel-strike; CTO, contralateral toe-off.

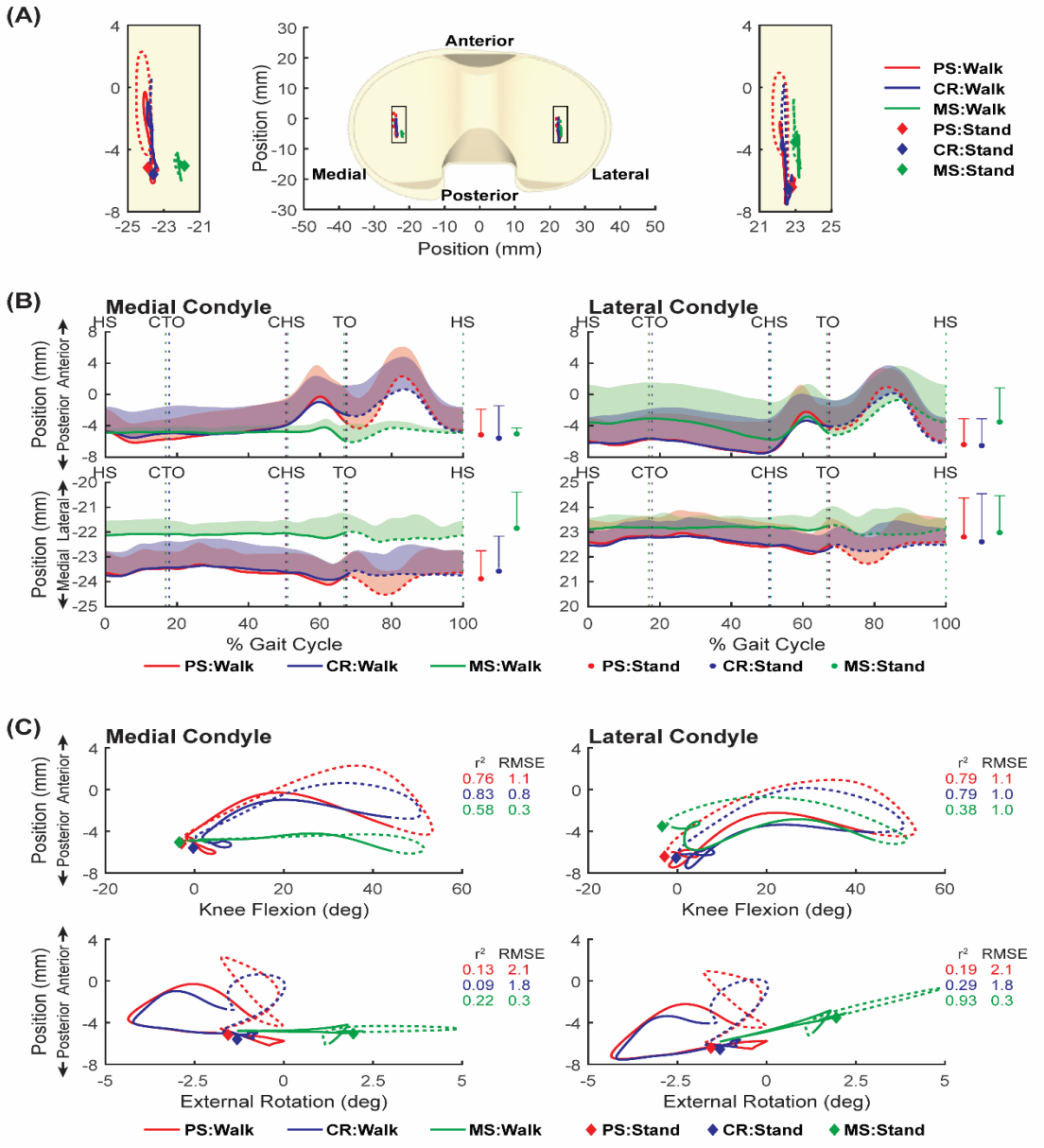

Fig. 10. Motion of femoral condylar centers relative to the tibia measured for standing and one cycle of overground walking for the prostheses compared to data previously reported by Gray et al.[26] for the healthy knee. Only mean data are shown for the prostheses: PS, posterior-stabilized; CR, cruciate-retaining; and MS, medial-stabilized. (A) Trajectories of the medial and lateral femoral condylar centers projected onto the tibial plateau for the healthy knee (top panel) and the prostheses (bottom panel; identical with Fig. 6A). The insets show magnified views of the motion trajectories. (B) Anterior-posterior translations of the condylar centers plotted against percentage of the gait cycle for the prosthetic knees and the healthy knee. The black solid lines represent the mean values measured for the healthy knee while the grey shaded areas represent ±1 standard deviation from the mean. Each dot and whisker on the far right-side of each panel represent the mean and ±1 standard deviation from the mean for standing for the prostheses and healthy knee. Solid lines represent the stance phase and dashed lines represent the swing phase. HS, heel-strike; TO, toe-off; CHS, contralateral heel-strike; CTO, contralateral toe-off.

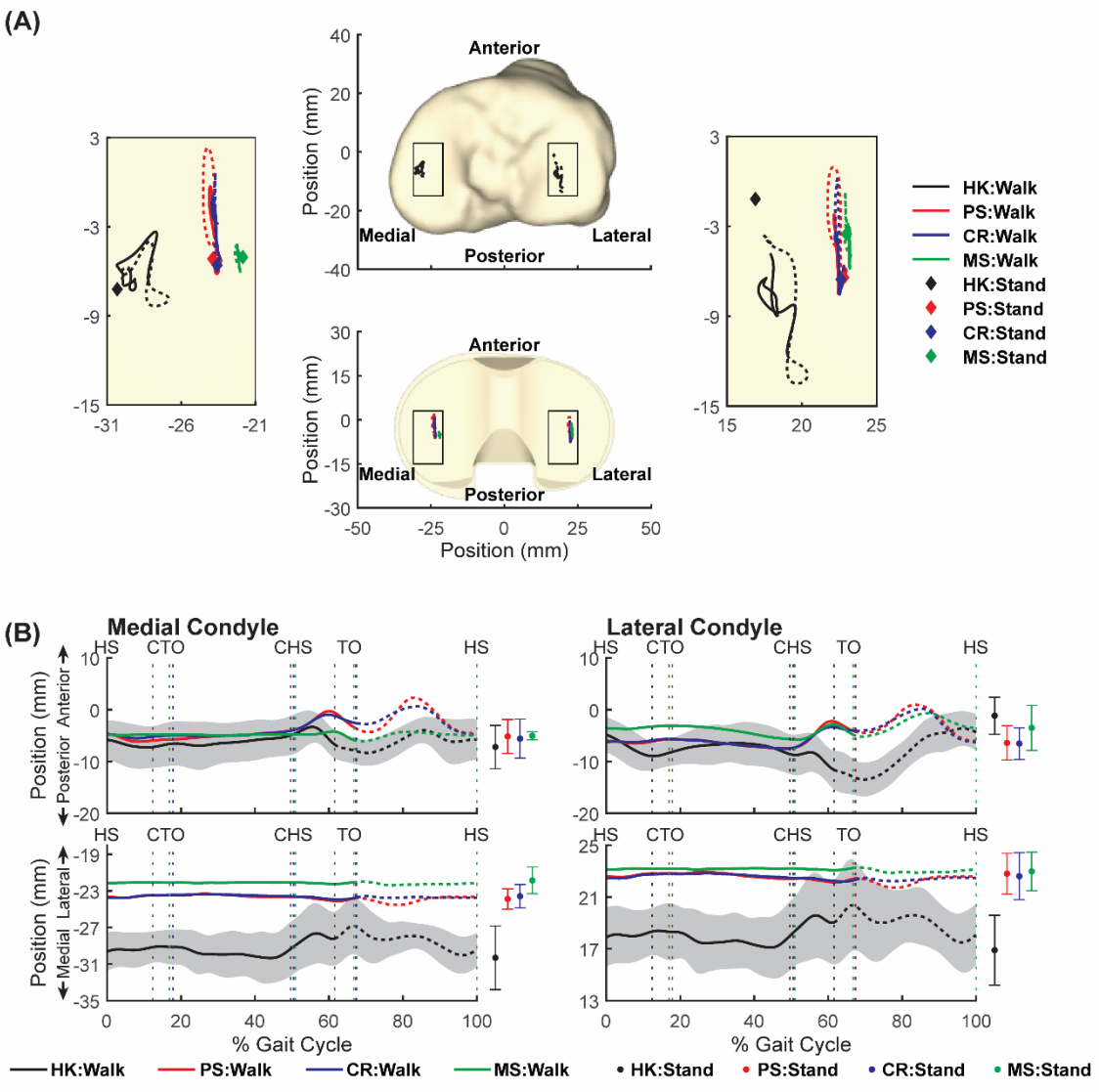

Tables

Table 1. Characteristics of the total knee arthroplasty patients from whom gait data were collected.

Group	Number of patients			Age	Surgery to testing	BMI	Height	Weight
	Gait experiments	Males	Females	(years)	(months)	(kg/m^2)	(cm)	(kg)
PS	23	14	9	66.8 ± 7.34	6.1 ± 0.8	30.9 ± 4.5	170.3 ± 8.8	89.4 ± 13.0
CR	25	16	9	71.5 ± 7.06	5.9 ± 1.2	31.2 ± 5.0	170.0 ± 12.5	89.6 ± 14.6
MS	26	12	14	67.3 ± 6.44	6.3 ± 0.9	33.8 ± 4.6	165.8 ± 10.0	93.1 ± 16.4

Table 2. Six-degree-of-freedom knee kinematic parameters measured for walking and standing. Data are presented for the entire gait cycle, stance phase only, and standing. Mean, maximum, minimum and peak-to-peak (PTP = maximum - minimum) values are given. Rotations and translations of the tibia relative to the femur are given in degrees and mm respectively. PS, posterior-stabilized; CR, cruciate-retaining; and MS, medial-stabilized.

	PS	CR	MS	P Val.	PS vs CR			PS vs MS			CR vs MS		
				(ANOVA)	Dif.	95% CI	P Val.	Dif.	95% CI	P Val.	Dif.	95% CI	P Val.
Comparisons between PS CR and MS kinematics for the entire gait cycle													
Mean Flexion	12.7	14.6	13.4	0.614	-1.9	-6.1 to 2.3		-0.7	-4.6 to 3.2		1.2	-2.4 to 4.8	
Mean Abduction	0.0	0.0	0.2	0.012 †	0.1	-0.1 to 0.2	0.433	-0.2	-0.4 to 0.0	0.031	-0.3	-0.4 to -0.1	**0.012** *
Mean External Rotation	-1.6	-1.8	1.6	0.040 †	0.2	-2.7 to 3.2	0.882	-3.1	-6.0 to -0.3	0.033	-3.3	-6.3 to -0.3	0.029
Mean Lateral Shift	0.5	0.4	0.2	0.050	0.1	-0.1 to 0.4		0.3	0.1 to 0.6		0.2	-0.1 to 0.5	
Mean Anterior Drawer	4.2	4.2	4.2	1.000	0.0	-1.3 to 1.3		0.0	-1.2 to 1.2		0.0	-1.3 to 1.3	
Mean Joint Distraction	0.2	0.1	-0.1	0.001 †	0.2	-0.1 to 0.4	0.145	0.3	0.2 to 0.5	**0.000** *	0.2	0.0 to 0.3	**0.010** *
Max Flexion	54.8	53.4	52.5	0.642	1.4	-3.6 to 6.4		2.3	-2.6 to 7.1		0.9	-3.8 to 5.5	
Max Abduction	1.4	1.0	1.9	0.025 †	0.4	-0.1 to 0.8	0.120	-0.4	-1.1 to 0.2	0.189	-0.8	-1.4 to -0.2	**0.012** *
Max External Rotation	2.7	2.9	6.2	0.036 †	-0.2	-3.3 to 2.9	0.904	-3.5	-6.2 to -0.8	**0.013** *	-3.3	-6.4 to -0.1	0.042
Max Lateral Shift	2.0	1.6	1.2	0.004 †	0.4	-0.1 to 0.9	0.128	0.8	0.4 to 1.2	**0.001** *	0.4	0.0 to 0.8	0.078
Max Anterior Drawer	7.3	6.7	6.4	0.460	0.6	-0.9 to 2.0		0.9	-0.5 to 2.3		0.4	-1.3 to 2.0	

Max Joint Distraction	1.1	0.9	0.7	0.023 †	0.2	-0.1 to 0.5	0.159	0.4	0.1 to 0.7	**0.008** *	0.2	-0.1 to 0.5	0.152
Min Flexion	-4.4	-1.4	-3.6	0.284	-3.0	-7.2 to 1.2		-0.8	-4.7 to 3.1		2.2	-1.3 to 5.6	
Min Abduction	-1.0	-0.8	-0.9	0.795	-0.1	-0.6 to 0.3		-0.1	-0.5 to 0.3		0.0	-0.4 to 0.5	
Min External Rotation	-5.3	-5.7	-2.7	0.122	0.3	-2.8 to 3.5		-2.7	-6.1 to 0.7		-3.0	-6.2 to 0.2	
Min Lateral Shift	-0.5	-0.5	-0.7	0.299	0.0	-0.4 to 0.3		0.3	-0.1 to 0.7		0.3	-0.2 to 0.7	
Min Anterior Drawer	-2.6	-1.0	2.0	0.000 †	-1.6	-2.9 to -0.3	0.019	-4.5	-5.8 to -3.3	**0.000** *	-3.0	-4.2 to -1.8	**0.000** *
Min Joint Distraction	-0.5	-0.5	-0.5	0.688	0.0	-0.1 to 0.2		0.1	-0.1 to 0.2		0.0	-0.1 to 0.2	
PTP Flexion	59.2	54.8	56.1	0.224	4.4	-0.8 to 9.6		3.1	-1.9 to 8.2		-1.3	-6.4 to 3.8	
PTP Abduction	2.4	1.9	2.7	0.033 †	0.5	0.0 to 1.1	0.067	-0.3	-1.0 to 0.4	0.347	-0.8	-1.5 to -0.2	**0.016** *
PTP External Rotation	8.0	8.6	8.8	0.739	-0.5	-2.5 to 1.5		-0.8	-2.8 to 1.3		-0.3	-2.4 to 1.8	
PTP Lateral Shift	2.5	2.1	1.9	0.125	0.4	-0.1 to 0.9		0.5	0.0 to 1.0		0.1	-0.4 to 0.6	
PTP Anterior Drawer	9.9	7.8	4.4	0.000 †	2.1	0.7 to 3.6	**0.004** *	5.5	4.2 to 6.8	**0.000** *	3.3	1.9 to 4.7	**0.000** *
PTP Joint Distraction	1.5	1.4	1.2	0.071	0.2	-0.1 to 0.4		0.4	0.0 to 0.7		0.2	-0.2 to 0.5	
Comparisons between PS CR and MS kinematics for stance phase													
Mean Flexion	5.0	8.0	6.7	0.376	-3.0	-7.5 to 1.6		-1.7	-6.0 to 2.6		1.3	-2.4 to 5.0	
Mean Abduction	-0.1	-0.1	0.2	0.023 †	0.0	-0.1 to 0.1	0.940	-0.2	-0.4 to 0.0	0.027	-0.2	-0.4 to 0.0	0.035
Mean External Rotation	-1.9	-2.1	1.0	0.060	0.2	-2.7 to 3.2		-2.9	-5.9 to 0.1		-3.2	-6.1 to -0.2	
Mean Lateral Shift	0.3	0.3	0.1	0.295	0.1	-0.2 to 0.3		0.2	-0.1 to 0.5		0.2	-0.2 to 0.5	
Mean Anterior Drawer	5.1	5.1	4.4	0.523	0.1	-1.4 to 1.6		0.7	-0.6 to 2.0		0.7	-0.8 to 2.1	
Mean Joint Distraction	0.1	0.0	-0.2	0.009 †	0.2	-0.1 to 0.4	0.165	0.3	0.1 to 0.5	**0.002** *	0.2	0.0 to 0.3	0.066
Max Flexion	45.1	44.4	44.4	0.949	0.7	-4.3 to 5.7		0.7	-4.6 to 6.0		0.0	-4.3 to 4.3	
Max Abduction	1.2	0.9	1.6	0.065	0.2	-0.3 to 0.7		-0.5	-1.2 to 0.2		-0.7	-1.4 to 0.0	
Max External Rotation	1.5	0.8	3.9	0.093	0.7	-2.3 to 3.8		-2.3	-5.0 to 0.4		-3.0	-6.1 to 0.0	
Max Lateral Shift	1.4	1.1	0.8	0.005 †	0.4	0.0 to 0.7	0.041	0.6	0.2 to 1.0	**0.003** *	0.2	-0.1 to 0.6	0.161
Max Anterior Drawer	7.1	6.7	6.1	0.383	0.5	-1.0 to 1.9		1.0	-0.3 to 2.4		0.6	-1.0 to 2.1	
Max Joint Distraction	0.9	0.7	0.5	0.022 †	0.2	-0.1 to 0.5	0.241	0.4	0.1 to 0.8	**0.011** *	0.3	0.0 to 0.5	0.084
Min Flexion	-3.3	-0.1	-2.1	0.278	-3.2	-7.7 to 1.2		-1.3	-5.4 to 2.8		2.0	-1.5 to 5.4	
Min Abduction	-0.6	-0.6	-0.4	0.271	0.0	-0.2 to 0.2		-0.2	-0.4 to 0.1		-0.2	-0.4 to 0.1	
Min External Rotation	-5.0	-5.2	-2.1	0.099	0.3	-2.9 to 3.5		-2.9	-6.3 to 0.5		-3.2	-6.4 to 0.1	
Min Lateral Shift	-0.4	-0.3	-0.5	0.582	0.0	-0.4 to 0.3		0.1	-0.2 to 0.5		0.2	-0.2 to 0.6	
Min Anterior Drawer	-0.3	0.8	3.0	0.000 †	-1.1	-2.2 to 0.1	0.062	-3.3	-4.6 to -2.1	**0.000** *	-2.2	-3.4 to -1.1	**0.000** *
Min Joint Distraction	-0.4	-0.5	-0.5	0.759	0.0	-0.1 to 0.2		0.1	-0.1 to 0.2		0.0	-0.1 to 0.2	
PTP Flexion	48.4	44.5	46.4	0.266	3.9	-1.1 to 8.9		2.0	-3.0 to 6.9		-1.9	-6.2 to 2.3	

PTP Abduction	1.8	1.6	2.1	0.212	0.2	-0.3 to 0.7		-0.3	-1.0 to 0.4		-0.5	-1.2 to 0.1		
PTP External Rotation	6.5	6.0	5.9	0.726	0.5	-1.0 to 2.0		0.6	-1.0 to 2.2		0.1	-1.4 to 1.6		
PTP Lateral Shift	1.8	1.4	1.3	0.036 †	0.4	0.0 to 0.8	0.042	0.5	0.1 to 0.8	**0.012** *	0.0	-0.3 to 0.4	0.797	
PTP Anterior Drawer	7.5	5.9	3.1	0.000 †	1.5	0.4 to 2.7	**0.007** *	4.4	3.4 to 5.3	**0.000** *	2.8	1.9 to 3.7	**0.000** *	
PTP Joint Distraction	1.3	1.2	1.0	0.050 †	0.2	-0.1 to 0.4	0.239	0.4	0.0 to 0.7	0.028	0.2	-0.1 to 0.5	0.159	
Comparisons between PS CR and MS kinematics for standing														
Mean Flexion	-2.9	-0.3	-3.5	0.389	-2.6	-7.8 to 2.7		0.5	-4.2 to 5.3		3.1	-1.6 to 7.8		
Mean Abduction	0.0	0.0	0.0	0.877	-0.1	-0.3 to 0.2		0.0	-0.2 to 0.2		0.0	-0.2 to 0.3		
Mean External Rotation	-1.6	-1.3	1.9	0.037 †	-0.3	-3.3 to 2.8	0.867	-3.5	-6.6 to -0.4	0.026	-3.3	-6.2 to -0.3	0.033	
Mean Lateral Shift	0.4	0.4	0.1	0.107	0.0	-0.3 to 0.3		0.2	0.0 to 0.5		0.3	0.0 to 0.6		
Mean Anterior Drawer	5.8	6.1	4.3	0.035 †	-0.4	-1.9 to 1.2	0.639	1.4	0.1 to 2.8	0.042	1.8	0.3 to 3.3	0.019	
Mean Joint Distraction	0.4	0.2	-0.1	0.011 †	0.2	-0.2 to 0.6	0.336	0.5	0.2 to 0.8	**0.000** *	0.3	0.0 to 0.6	0.053	

Statistical significance: † indicates $p < 0.05$ for ANOVA; *** Bold type** indicates $p < 0.017$ for t-tests

Table 3. Motion of the centers of the medial and lateral femoral condyles measured for walking and standing. Data are presented for the entire gait cycle, stance phase only, and standing. Mean, maximum, minimum and peak-to-peak (PTP = maximum - minimum) values are given. Anterior-posterior and medial-lateral translations of the femoral condylar centers are given in mm. All results are expressed in the tibial reference frame (see Figs. 3 and 6A).

					PS vs CR			PS vs MS			CR vs MS		
	PS	CR	MS	P Val. (ANOVA)	Dif.	95% CI	P Val.	Dif.	95% CI	P Val.	Dif.	95% CI	P Val.
Comparisons between PS CR and MS kinematics for the entire gait cycle													
Mean Lat Trans on Med Condyle	-24.0	-23.6	-21.9	0.000 †	-0.4	-1.1 to 0.3	0.285	-2.1	-2.8 to -1.3	**0.000** *	-1.7	-2.4 to -0.9	**0.000** *
Mean Ant Trans on Med Condyle	-3.6	-3.6	-4.8	0.129	-0.1	-1.8 to 1.7		1.2	0.0 to 2.3		1.3	0.0 to 2.5	
Mean Lat Trans on Lat Condyle	22.7	22.5	22.9	0.746	0.2	-0.8 to 1.1		-0.2	-1.0 to 0.7		-0.3	-1.3 to 0.6	
Mean Ant Trans on Lat Condyle	-4.9	-4.9	-3.6	0.323	-0.1	-1.8 to 1.7		-1.3	-3.4 to 0.7		-1.3	-3.4 to 0.9	
Max Lat Trans on Med Condyle	-23.0	-22.7	-21.1	0.000 †	-0.3	-1.1 to 0.4	0.362	-1.9	-2.8 to -1.1	**0.000** *	-1.6	-2.4 to -0.8	**0.000** *
Max Ant Trans on Med Condyle	3.7	1.8	-3.7	0.000 †	2.0	-0.2 to 4.1	0.074	7.4	5.8 to 8.9	**0.000** *	5.4	3.9 to 6.9	**0.000** *
Max Lat Trans on Lat Condyle	23.7	23.4	23.7	0.814	0.2	-0.8 to 1.2		0.0	-0.9 to 0.8		-0.3	-1.3 to 0.7	
Max Ant Trans on Lat Condyle	1.8	1.0	0.3	0.265	0.8	-0.9 to 2.4		1.5	-0.3 to 3.3		0.7	-1.2 to 2.7	
Min Lat Trans on Med Condyle	-25.3	-24.6	-22.8	0.000 †	-0.7	-1.6 to 0.1	0.097	-2.5	-3.4 to -1.6	**0.000** *	-1.8	-2.6 to -0.9	**0.000** *

Min Ant Trans on Med Condyle	-7.3	-6.4	-6.6	0.506	-0.9	-2.7 to 0.9		-0.7	-2.2 to 0.8		0.2	-1.3 to 1.8		
Min Lat Trans on Lat Condyle	21.4	21.4	21.9	0.461	0.0	-0.9 to 1.0		-0.5	-1.3 to 0.4		-0.5	-1.4 to 0.4		
Min Ant Trans on Lat Condyle	-8.7	-7.9	-7.0	0.331	-0.8	-2.9 to 1.3		-1.7	-4.1 to 0.6		-0.9	-3.4 to 1.5		
PTP Lat Trans on Med Condyle	2.3	1.9	1.7	0.053	0.4	0.0 to 0.8		0.6	0.1 to 1.0		0.2	-0.3 to 0.6		
PTP Ant Trans on Med Condyle	11.1	8.2	3.0	0.000 †	2.9	1.3 to 4.5	**0.001** *	8.1	6.5 to 9.6	**0.000** *	5.2	3.7 to 6.7	**0.000** *	
PTP Lat Trans on Lat Condyle	2.2	2.0	1.8	0.193	0.2	-0.2 to 0.7		0.4	0.0 to 0.9		0.2	-0.3 to 0.7		
PTP Ant Trans on Lat Condyle	10.5	8.9	7.3	0.002 †	1.6	-0.1 to 3.2	0.069	3.2	1.5 to 4.9	**0.000** *	1.7	-0.2 to 3.5	0.079	
Comparisons between PS CR and MS kinematics for stance phase														
Mean Lat Trans on Med Condyle	-23.8	-23.5	-21.9	0.00 †	-0.3	-1.0 to 0.4	0.393	-2.0	-2.7 to -1.2	**0.000** *	-1.6	-2.4 to -0.9	**0.000** *	
Mean Ant Trans on Med Condyle	-4.4	-4.2	-4.8	0.72	-0.2	-2.0 to 1.6		0.4	-0.9 to 1.6		0.6	-0.7 to 1.9		
Mean Lat Trans on Lat Condyle	22.8	22.6	22.9	0.76	0.2	-0.7 to 1.2		-0.1	-0.9 to 0.7		-0.3	-1.3 to 0.6		
Mean Ant Trans on Lat Condyle	-6.0	-5.8	-4.0	0.12	-0.2	-2.1 to 1.8		-2.0	-4.2 to 0.2		-1.8	-4.1 to 0.4		
Max Lat Trans on Med Condyle	-23.1	-22.8	-21.4	0.00 †	-0.3	-1.1 to 0.4	0.421	-1.8	-2.6 to -1.0	**0.000** *	-1.5	-2.3 to -0.7	**0.000** *	
Max Ant Trans on Med Condyle	1.3	0.6	-3.8	0.00 †	0.7	-1.2 to 2.7	0.459	5.1	3.6 to 6.6	**0.000** *	4.4	3.1 to 5.6	**0.000** *	
Max Lat Trans on Lat Condyle	23.6	23.3	23.5	0.83	0.3	-0.7 to 1.3		0.1	-0.7 to 0.9		-0.2	-1.1 to 0.8		
Max Ant Trans on Lat Condyle	-0.6	-1.8	-1.7	0.31	1.3	-0.2 to 2.7		1.1	-0.8 to 3.1		-0.1	-2.1 to 1.8		
Min Lat Trans on Med Condyle	-24.8	-24.3	-22.5	0.00 †	-0.5	-1.4 to 0.4	0.261	-2.3	-3.2 to -1.4	**0.000** *	-1.8	-2.7 to -0.9	**0.000** *	
Min Ant Trans on Med Condyle	-6.9	-6.3	-6.2	0.57	-0.7	-2.5 to 1.1		-0.7	-2.0 to 0.6		0.0	-1.5 to 1.4		
Min Lat Trans on Lat Condyle	21.9	21.8	22.3	0.48	0.1	-0.8 to 0.9		-0.4	-1.2 to 0.4		-0.5	-1.4 to 0.4		
Min Ant Trans on Lat Condyle	-8.6	-7.9	-6.6	0.23	-0.7	-2.9 to 1.4		-2.0	-4.3 to 0.4		-1.2	-3.7 to 1.2		
PTP Lat Trans on Med Condyle	1.6	1.4	1.1	0.02 †	0.2	-0.2 to 0.5	0.284	0.5	0.2 to 0.8	**0.005** *	0.3	-0.1 to 0.7	0.104	
PTP Ant Trans on Med Condyle	8.2	6.8	2.4	0.00 †	1.4	0.2 to 2.6	0.022	5.8	4.6 to 7.0	**0.000** *	4.4	3.3 to 5.5	**0.000** *	
PTP Lat Trans on Lat Condyle	1.7	1.5	1.2	0.03 †	0.2	-0.2 to 0.6	0.299	0.5	0.2 to 0.8	**0.005** *	0.3	-0.1 to 0.7	0.114	
PTP Ant Trans on Lat Condyle	8.0	6.0	4.9	0.00 †	2.0	0.6 to 3.3	**0.005** *	3.1	1.9 to 4.3	**0.000** *	1.1	0.0 to 2.2	0.058	
Comparisons between PS CR and MS kinematics for standing														
Mean Lat Trans on Med Condyle	-23.9	-23.6	-21.8	0.00 †	-0.3	-1.0 to 0.4	0.387	-2.0	-2.8 to -1.3	**0.000** *	-1.7	-2.5 to -1.0	**0.000** *	
Mean Ant Trans on Med Condyle	-5.2	-5.6	-5.0	0.78	0.4	-1.6 to 2.5		-0.1	-1.5 to 1.2		-0.5	-2.1 to 1.0		
Mean Lat Trans on Lat Condyle	22.8	22.6	23.0	0.73	0.2	-0.8 to 1.2		-0.2	-1.1 to 0.7		-0.4	-1.3 to 0.6		
Mean Ant Trans on Lat Condyle	-6.4	-6.5	-3.5	0.01 †	0.1	-1.7 to 2.0	0.894	-2.9	-5.2 to -0.7	**0.012** *	-3.0	-5.2 to -0.9	**0.006** *	

Statistical significance: † indicates $p < 0.05$ for ANOVA; * **Bold type** indicates $p < 0.017$ for t-tests

Table 4. Motion of the contact centers in the medial and lateral compartments of the tibiofemoral joint measured for walking and standing. Data are presented for the entire gait cycle, stance phase only, and standing. Mean, maximum, minimum and peak-to-peak (PTP = maximum - minimum) values are given. Anterior-posterior and medial-lateral translations of the tibiofemoral contact centers are given in mm. All results are expressed in the tibial reference frame (see Figs. 3 and 7A).

				P Val.	PS vs CR			PS vs MS			CR vs MS		
	PS	CR	MS	(ANOVA)	Dif.	95% CI	P Val.	Dif.	95% CI	P Val.	Dif.	95% CI	P Val.
Comparisons between PS CR and MS kinematics for the entire gait cycle													
Mean Lat Trans on Med Condyle	-23.2	-23.3	-22.9	0.651	0.1	-0.9 to 1.2		-0.3	-1.0 to 0.5		-0.4	-1.3 to 0.5	
Mean Ant Trans on Med Condyle	-1.9	-2.4	-4.9	0.000 †	0.5	-1.0 to 1.9	0.516	3.0	2.0 to 3.9	**0.000** *	2.5	1.4 to 3.6	**0.000** *
Mean Lat Trans on Lat Condyle	22.4	22.8	25.3	0.000 †	-0.4	-1.4 to 0.5	0.398	-2.9	-3.9 to -1.9	**0.000** *	-2.5	-3.5 to -1.5	**0.000** *
Mean Ant Trans on Lat Condyle	-3.2	-4.0	-3.1	0.553	0.9	-0.5 to 2.3		-0.1	-2.1 to 2.0		-0.9	-3.0 to 1.2	
Max Lat Trans on Med Condyle	-21.9	-22.3	-21.6	0.253	0.5	-0.6 to 1.6		-0.3	-1.1 to 0.5		-0.8	-1.7 to 0.2	
Max Ant Trans on Med Condyle	3.1	1.4	-3.5	0.000 †	1.7	-0.3 to 3.8	0.099	6.6	5.2 to 8.1	**0.000** *	4.9	3.4 to 6.4	**0.000** *
Max Lat Trans on Lat Condyle	24.4	24.6	26.6	0.000 †	-0.2	-1.1 to 0.7	0.702	-2.2	-3.2 to -1.2	**0.000** *	-2.0	-2.9 to -1.1	**0.000** *
Max Ant Trans on Lat Condyle	1.5	0.2	1.1	0.380	1.3	-0.2 to 2.7		0.4	-1.5 to 2.4		-0.8	-2.8 to 1.2	
Min Lat Trans on Med Condyle	-25.1	-24.7	-24.1	0.133	-0.4	-1.6 to 0.7		-1.0	-1.7 to -0.2		-0.6	-1.6 to 0.4	
Min Ant Trans on Med Condyle	-6.8	-5.7	-6.9	0.210	-1.0	-2.7 to 0.6		0.1	-1.2 to 1.5		1.2	-0.2 to 2.6	
Min Lat Trans on Lat Condyle	19.9	20.4	23.5	0.000 †	-0.5	-1.5 to 0.4	0.257	-3.6	-4.7 to -2.5	**0.000** *	-3.1	-4.2 to -2.0	**0.000** *
Min Ant Trans on Lat Condyle	-6.8	-6.8	-7.2	0.904	0.0	-1.6 to 1.7		0.4	-1.9 to 2.8		0.4	-2.0 to 2.8	
PTP Lat Trans on Med Condyle	3.3	2.4	2.6	0.010 †	0.9	0.3 to 1.5	**0.007** *	0.7	0.1 to 1.3	0.023	-0.2	-0.7 to 0.4	0.487
PTP Ant Trans on Med Condyle	9.9	7.1	3.4	0.000 †	2.8	1.3 to 4.3	**0.000** *	6.5	5.0 to 8.0	**0.000** *	3.7	2.5 to 4.9	**0.000** *
PTP Lat Trans on Lat Condyle	4.6	4.2	3.1	0.000 †	0.4	-0.2 to 1.0	0.206	1.4	0.9 to 2.0	**0.000** *	1.1	0.6 to 1.6	**0.000** *
PTP Ant Trans on Lat Condyle	8.3	7.1	8.3	0.211	1.2	0.0 to 2.5		0.0	-1.7 to 1.8		-1.2	-2.9 to 0.5	
Comparisons between PS CR and MS kinematics for stance phase													
Mean Lat Trans on Med Condyle	-23.0	-23.2	-22.8	0.65	0.3	-0.8 to 1.3		-0.1	-0.9 to 0.6		-0.4	-1.3 to 0.5	
Mean Ant Trans on Med Condyle	-2.2	-2.8	-4.8	0.00 †	0.6	-0.8 to 2.0	0.386	2.7	1.7 to 3.7	**0.000** *	2.1	1.0 to 3.1	**0.000** *
Mean Lat Trans on Lat Condyle	22.4	22.8	25.3	0.00 †	-0.4	-1.4 to 0.6	0.422	-2.9	-3.9 to -1.9	**0.000** *	-2.5	-3.5 to -1.5	**0.000** *
Mean Ant Trans on Lat Condyle	-3.7	-4.7	-3.4	0.41	1.0	-0.5 to 2.5		-0.2	-2.4 to 2.0		-1.2	-3.5 to 1.0	
Max Lat Trans on Med Condyle	-22.0	-22.5	-21.8	0.36	0.4	-0.6 to 1.5		-0.2	-1.0 to 0.6		-0.6	-1.6 to 0.3	
Max Ant Trans on Med Condyle	1.0	0.0	-3.6	0.00 †	1.0	-0.8 to 2.7	0.267	4.6	3.4 to 5.9	**0.000** *	3.7	2.5 to 4.9	**0.000** *
Max Lat Trans on Lat Condyle	24.3	24.5	26.4	0.00 †	-0.2	-1.1 to 0.8	0.696	-2.2	-3.2 to -1.2	**0.000** *	-2.0	-2.9 to -1.1	**0.000** *

Max Ant Trans on Lat Condyle	-0.8	-2.5	-0.7	0.10	1.7	0.4 to 3.1		-0.1	-2.1 to 2.0		-1.8	-3.9 to 0.3	
Min Lat Trans on Med Condyle	-24.5	-24.3	-23.7	0.20	-0.2	-1.3 to 0.8		-0.8	-1.6 to 0.0		-0.6	-1.5 to 0.4	
Min Ant Trans on Med Condyle	-6.1	-5.4	-6.5	0.24	-0.7	-2.3 to 0.9		0.4	-0.7 to 1.6		1.1	-0.1 to 2.4	
Min Lat Trans on Lat Condyle	20.4	20.8	23.8	0.00 †	-0.4	-1.4 to 0.6	0.389	-3.5	-4.5 to -2.4	**0.000** *	-3.0	-4.1 to -2.0	**0.000** *
Min Ant Trans on Lat Condyle	-6.4	-6.8	-6.8	0.94	0.3	-1.2 to 1.9		0.3	-2.0 to 2.7		0.0	-2.4 to 2.4	
PTP Lat Trans on Med Condyle	2.5	1.8	1.9	0.06	0.7	0.0 to 1.3		0.6	0.0 to 1.2		-0.1	-0.6 to 0.5	
PTP Ant Trans on Med Condyle	7.1	5.5	2.9	0.00 †	1.6	0.6 to 2.7	**0.003** *	4.2	3.1 to 5.3	**0.000** *	2.6	1.7 to 3.4	**0.000** *
PTP Lat Trans on Lat Condyle	3.9	3.7	2.6	0.00 †	0.2	-0.4 to 0.9	0.451	1.3	0.7 to 1.9	**0.000** *	1.1	0.5 to 1.6	**0.000** *
PTP Ant Trans on Lat Condyle	5.6	4.2	6.0	0.00 †	1.4	0.6 to 2.2	**0.001** *	-0.4	-1.5 to 0.7	0.475	-1.8	-2.8 to -0.8	**0.001** *
Comparisons between PS CR and MS kinematics for standing													
Mean Lat Trans on Med Condyle	-23.1	-23.3	-22.8	0.50	0.2	-0.8 to 1.3		-0.3	-1.1 to 0.5		-0.5	-1.5 to 0.4	
Mean Ant Trans on Med Condyle	-1.3	-2.5	-5.1	0.00 †	1.3	-0.4 to 2.9	0.133	3.9	2.8 to 5.0	**0.000** *	2.6	1.4 to 3.9	**0.000** *
Mean Lat Trans on Lat Condyle	22.9	23.2	25.1	0.00 †	-0.3	-1.3 to 0.8	0.609	-2.2	-3.3 to -1.2	**0.000** *	-2.0	-3.1 to -0.9	**0.001** *
Mean Ant Trans on Lat Condyle	-2.5	-3.8	-1.8	0.12	1.3	-0.1 to 2.7		-0.7	-3.0 to 1.5		-2.0	-4.2 to 0.2	

Statistical significance: † indicates $p < 0.05$ for ANOVA; *** Bold type** indicates $p < 0.017$ for t-tests